A ES
ISSN: 2096-3246
Volume 58, Issue 01, 2026

STRUCTURAL AND LUMINESCENCE PROPERTIES OF RARE EARTH INFUSED BOROBISMUTH GLASSES FOR PHOTONIC APPLICATIONS

Kiran D S , Susheela K Lenkennavar *
Department of Physics, Bangalore University, Bengaluru, Karnataka, 560056, India.
Email: kiran1998ds@gmail.com and susheelakl@bub.ernet.in

Abstract
Rare earth infused Borobismuth glasses were synthesized using traditional melt quenching experimental method to study their structural and luminescence properties. Amorphous nature of the samples was confirmed by X-ray diffraction and Raman analysis revealed progressive recognization of borate structural units resulting in modified network connectivity. The observed variations in density, optical polarizability, and related physical and optical parameters confirm the stabilization of the glass network compactness. Photoluminescence (PL) investigations showed broad ultraviolet visible emission with intensity modulation controlled by heavy metaloxide and rare earth concentration. An improvement in emission efficiency at lower concentrations is associated with enhanced structural asymmetry and stronger local field effects, whereas luminescence quenching at higher concentration is linked to increase the non radiative energy transfer. These findings indicate that the prepared rare earth infused borobismuth glasses may be used in solid state lighting and advanced photonic applications.
Keywords: Borobismuth glasses, Optical polarizability, Photoluminescence, Photonic applications.

1. Introoduction

Recently, rare earth glasses containing heavy metal oxides have attracted much attention from researchers due to their excellent optical performance and structural flexibility for photonic and optoelectronic applications. In particular, borobismuth glass systems are the most suitable materials due to their high refractive index, high density, strong optical basicity, and broad transparency from the visible to the near-infrared region. The chemical composition of the glass controls the physical and optical properties of the glass and short-range structural organization enabling effective tuning of these characteristics through compositional modification [1-2].
The most commonly used glass former is Boron oxide (B_2O_3) which has low melting point, high transparency, and chemical durability. In these borate glasses coexistence of BO_3 and BO_4 structural units provide considerable compositional flexibility and plays a vital role in modifying the structural and optical properties of borate glasses [3].
Bismuth oxide (Bi_2O_3) is an environmentally friendly alternative to lead oxide, inocorporation of this into the glass enhances refractive index, ionic polarizability, and visible near infrared transmission through the formation of BiO_3 and BiO_6 units [4-7]. Generally, alkali metaloxides act as a network modifier, for instant sodium oxide (Na_2O) create non-bridging oxygens [NBOs] that

influence glass compactness and optical absorption, while transition metaloxide like zinc oxide (ZnO), acting as an intermediate, improves glass forming ability and thermal stability [8-10].
The infusion of rare earth oxides like La_2O_3, modifies the glass network due to the high field strength of La^{3+} ions, improved physical and optical properties [11]. Apart from conventional optical characteristics, the photoluminescence behavior of rare earth infused borobismuth glasses is crucial for photonic applications. Luminescence efficiency is strongly influenced by the local structural environment, phonon energy, and glass network rigidity, with B_2O_3 playing a significant role in enhancing radiative transitions [12-15]. Therefore, the present work focuses on the systematic synthesis of lanthanum infused borobismuth glasses to investigate structural and luminescence properties to assess their potential for advanced photonic applications.

2. Methadology

2.1 Material synthesis:

Table 1. illustrates the composition of the rare earth infused borobismuth glasses, which were prepared by the conventional melt quesnching experimental technique using analytical grade chemicals with purity 99.99%. The matrix of the synthesized glasses is $10ZnO\text{-}12Na_2O\text{-}(8+x)Bi_2O_3\text{-}yLa_2O_3\text{-}(70\text{-}x\text{-}y)B_2O_3$, where (x= 0, 2, 4, 6, 8 mol% and y=0, 0.5, 1.0, 1.5, 2.0 mol%). About 10 gm batches of the selected glass composition were accurately weighed and finely grinded it using an agate mortar to ensure homogeneity. The finely powders were melted in a procelain crucible at 850^0 C using an electrical muffle furnace. The molten liquid was poured into a preheated brass mould and annealed at 300^0 C for 3 hours to minimize the thermal stress, suppress air bubble formation, and enhance the mechanical strength. Then the samples were polished on both side to obtain flat surfaces, and labelled them as LB-0, LB-0.5, LB-1.0, LB-1.5, LB-2.0 as shown in the Figure 1.

Table 1. *composition of the prepared LB glasses*

Glass	LB-0	LB-	LB-	LB-	LB-
ZnO	10	10	10	10	10
Na_2O	12	12	12	12	12
Bi_2O_3	8	10	12	14	16
La_2O_3	0	0.5	1.0	1.5	2.0
B_2O_3	70	67.5	65	62.5	60

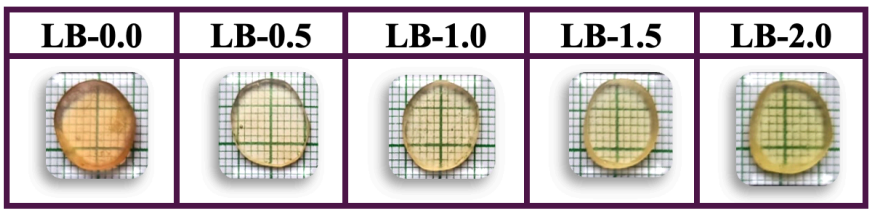

Figure 1. *synthesized LB glasses*

2.2 Physical and optical properties:

Density (ρ) g/cm^3, Refractive index (n), Transmission (T), Metallization (M), Optical electronegativity (χ), Electronic Polarizability (α_e), Optical basicity (Λ), Optical dielectric constant (ε') were calculated by applying the equations (1) to (9) [16].

$$\rho = \left(\frac{Wa}{Wa-Wb}\right) \rho_b \quad (1)$$

$$\frac{n^2-1}{n^2+2} = 1 - \sqrt{\frac{E_g}{20}} \quad (2)$$

$$T = \frac{2n}{(n^2+1)} \quad (3)$$

$$M = 1 - \left(\frac{R_m}{V_m}\right) \quad (4)$$

$$\chi = 0.2688 * E_g \quad (5)$$

$$\alpha_e = \frac{3}{4\pi N_A} \times R_m \quad (6)$$

$$\Lambda = -0.5 * \chi + 1.7 \quad (7)$$

$$\varepsilon' = n^2 - 1 \quad (8)$$

Where, W_a and W_b are weight of glass in air and toluene respectively, ρ_b is density of the toluene, E_g is optical energy band gap, R_m is Molar refractivity, V_m is Molar volume.

The optical properties were investigated using a UV-Visible absorption spectrophotometer (UV-T-7200 model) operating in the wavelength range of 200-1200 nm. The optical band gap energy (E_g) was evaluated by poltting tauc plots and using the following equation (9) [17], and Photoluminescence spectra of the prepared glass samples were recorded using a photoluminescence spectrophotometer equipped with a 150 W xenon lamp as the excitation source, a double monochromator, and a photomultiplier tube detector.

$$(\alpha h\nu)^n = A(h\nu - E_g) \quad (9)$$

Where, where α is the optical absorption coefficient, hν is the photon energy, A is a proportionality constant, and n denotes the nature of the electronic transition, n=2 for direct band gap and n=0.5 for the indirect band gap.

2.3 Structural properties:

2.3.1 X-ray diffraction and Raman spectroscopy:

X-ray diffraction (XRD) is a widely used technique to examine the structural nature of materials and to distinguish between amorphous and crystalline phases. In the present work, the XRD patterns of the prepared glass samples were recorded using an X-ray diffractometer with Cu-Kα radiation (λ = 1.5406 Å), operated at an accelerating voltage of 40 kV and a current of 30 mA. The

obtained diffraction patterns exhibited a broad diffuse hump without any sharp Bragg peaks, confirming the amorphous nature of the synthesized glass samples.

Raman spectroscopy was employed as a complementary, non-destructive technique to investigate the short-range structural order and vibrational characteristics of the glass network. The Raman spectra were recorded at room temperature in the spectral range of 200-1600 cm^{-1} using a Raman spectrometer with laser excitation. The observed Raman bands were analyzed to identify the presence of various structural units and to understand the influence of dopant concentration on the glass network connectivity.

3. Result and discussion

3.1. *structual properties:*

The X-ray diffraction pattern of the LB-2.0 glass sample as shown in Figure 2, represents the typical structural behavior of all prepared LB glass samples, as similar diffraction features were observed for every glass samples. The presence of two broad diffuse humps around $2\theta \approx 25\text{-}30°$ and 40-50°, along with the complete absence of sharp peaks, which clearly demonstrates the amorphous nature of the synthesized glass samples. These broad halos arise from the short and intermediate range ordering present in the glass network rather than long range periodicity. The diffuse hump at lower angles is attributed to the borate structural units, while the higher angle hump reflects intermediate range correlations within the glass matrix [18].

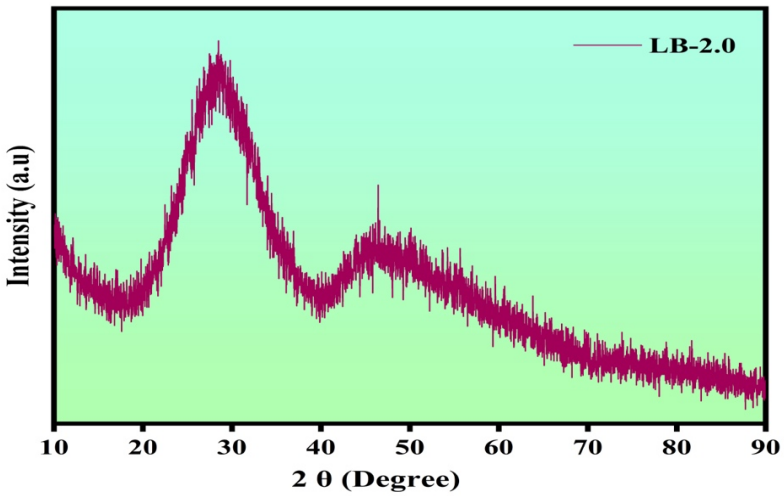

Figure 2. *XRD pattern of the LB-2.0 glass samples*

Table 2. and Figure 3. explains that the typical raman spectrum of the LB-2.0 glass sample exhibits broad and overlapping bands, which is a characteristic feature of amorphous glassy materials. The absence of sharp and well-defined raman peaks indicates the lack of long-range periodic structural order in the glass network. A band was observed in the region 300-350 cm^{-1}, which indicates that stretching vibrations of La-O bond [19]. The band observed in the region of 900-1100 cm^{-1} is attributed to vibrational bands arise from isolated diborate structural units and alkali metal-oxygen (M-O) bond vibrations, confirming the presence of four-coordinated boron and sodium in the

structure. The dominant broad band extending from 1200 to 1450 cm^{-1} corresponds to the asymmetric stretching vibrations of B-O bonds in trigonal BO_3 units, which form the backbone of the borate glass network. The prominence of this band suggests that BO_3 units play a major role in determining the structural framework of the LB glass system. In the region of higher wavenumber around 1500-1700 cm^{-1} appeariing two weak peaks which are related to distorted BO_3 units and BO_2O^- groups, and these indicate that the formation of non-bridging oxygen sites [20]. The extensive broadening and overlap of all Raman features reflect a high degree of structural disorder within the glass matrix.

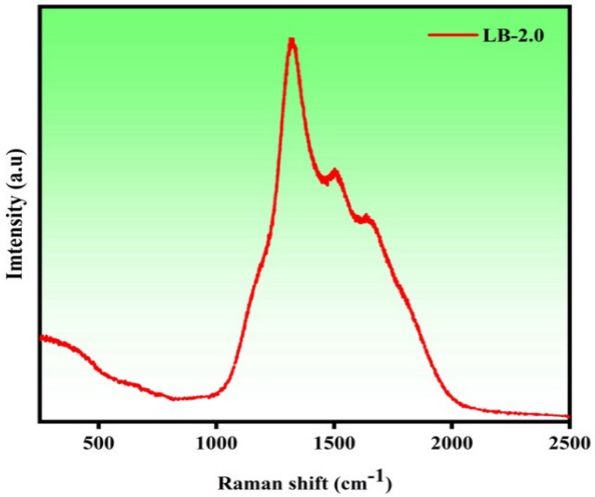

Figure 3. *Raman spectra of LB-2.0 glass sample*

Table 2. *Raman band assignments of LB glass samples*

Raman shift range (cm^{-1})	**Band assignments**
300-350	Stretching of La-O bond
900-1100	vibrational bands arise from isolated diborate structural units and alkali metal-oxygen (M-O) bond vibrations
1200-1450	Asymmetric stretching vibrations of B-O bonds in trigonal BO_3 units
1500-1700	Vibrations of distorted BO_3 units and BO_2O^- groups

3.2. Physical and Optical properties:

As varying the bismuth and lanthanum oxides in the glass system, a systematic variation can be observed in the physical and optical properties of the prepared LB galss samples which are listed in Table 3. These results highlight that the strong influence on the structure and optical response of the glasses because of heavy atomic mass and large ionic radii of the bismuth and lanthanum. Density of the LB glasses steadily incresed from 3.39 g/cm^3 (LB-0) to 4.44 g/cm^3 (LB-2.0) due to the La^{3+} and Bi^{3+} ions, which significantly increase the mass of the glass system. As well molar volume also increased because of large ionic radii of these ions, which indicates that an expansion of the glass network, this expansion arises from increased bond lengths and the formation of non-

bridging oxygen (NBO) sites. This behavior is typical of heavy-metal-oxide-based glass systems [21].

Figure 4. explains that a gradual increase of refractive index from 2.31 to 2.36 and electronic polarizability (α_e) from 7.02 to 7.45x10^{-24} cm^3 with increasing dopent concentration due to highly polarizable La^{3+} and Bi^{3+} ions, as well as increased NBO concentration, which boosts the light-matter interaction within the.In contrast, the optical transmission decreases slightly from 0.729 to 0.718, which can be attributed to increased absorption and scattering losses caused by heavy ions and enhanced structural disorder [22].

As increasing with dopant concentration metallization parameter (M) decreased from 0.409 to 0.396, which confirms that all LB galss samples retain their insulating nature. The decrease in metallization indicates increased electron localization and bond covalency rather than any tendency toward metallic behavior. Optical electronegativity (χ) shows a same decreasing trend, which reduced from 0.892 to 0.839, suggesting reduced bond ionicity and increased distortion of the electron cloud due to the presence of heavy, highly polarizable ions [16, 22].

optical basicity (Λ) from 1.253 to 1.281 trend can be seen in Figure 5, indicating an increase in oxide ion donor ability and the formation of a higher concentration of NBOs. These structural changes contribute directly to the observed increase in the optical dielectric constant (ε') from 4.34 to 4.57, demonstrating an improved dielectric response and enhanced ability of the glass to store electromagnetic energy [23-25].

Totally, the results presented in Table 3. clearly demonstrate that the incorporation of La^{3+} and Bi^{3+} ions lead to simultaneous increases in density, polarizability, optical basicity, and dielectric constant, while maintaining the insulating and amorphous nature of the LB glasses. These tunable physical and optical characteristics make the LB glass system a promising candidate for advanced optical and photonic applications.

Table 3. *Physical and optical properties of the LB Glass Samples*

Glass Samples	**LB-0**	**LB-0.5**	**LB-1.0**	**LB-1.5**	**LB-2.0**
Density (ρ) (g/cm^3)	3.39	3.69	3.93	4.22	4.44
Refractive index (n)	2.31	2.32	2.33	2.35	2.36
Transmission (T)	0.729	0.727	0.725	0.721	0.718
Metalization (M)	0.409	0.406	0.403	0.399	0.396
Optical electronegativity (χ)	0.892	0.887	0.871	0.855	0.839
Electronic polarizability (α_e)x10^{-24} (cm^3)	7.02	7.05	7.22	7.29	7.45
Optical basicity (Λ)	1.253	1.256	1.264	1.273	1.281
Optical dielectric constant (ε')	4.34	4.38	4.43	4.52	4.57

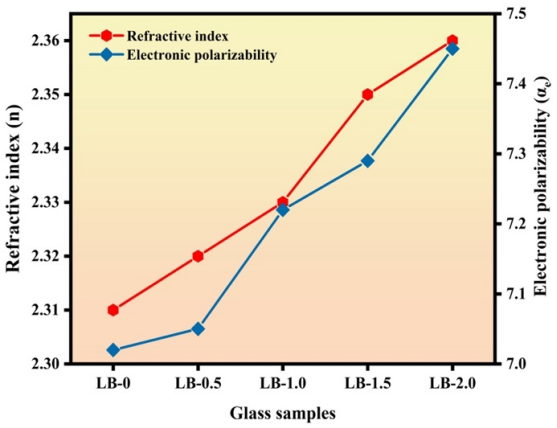

Figure 4.

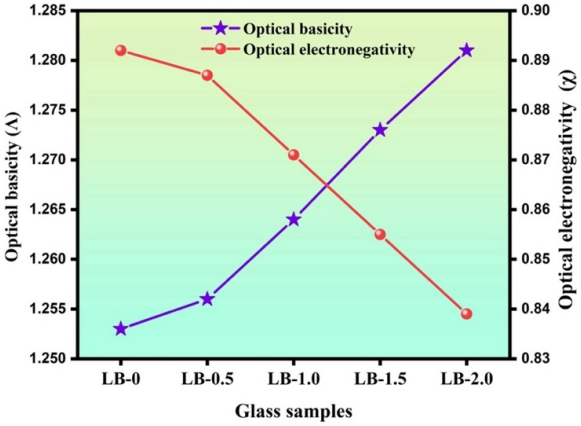

Figure 5.

Figure 4. *Refractive index and electronic polarizability and* ***Figure 5.*** *Optical basicity and Optical electronegativity of LB glass samples*

The UV-Visible absorption spectra of the LB glass samples shown in Figure 6. All glasses exhibit strong absorption in the ultraviolet region followed by a sharp absorption edge and high transparency in the visible region, indicating good optical homogeneity of the prepared samples. As increasing LB content from LB-0.0 to LB-2.0, a systematic red shift of the absorption edge toward longer wavelengths is clearly observed. This shift is accompanied by a gradual decrease in the optical band gap values. The direct optical band gap decreases from 3.323 eV (LB-0.0) to 3.120 eV (LB-2.0), while the indirect band gap reduces from 3.193 eV to 2.938 eV over the same compositional range. The decreasing of the optical energy band gaps is attributed to structural modifications within the glass network, where the incorporation of Bi-O and La-O bonds replace B-O-B linkages, promotes the formation of NBO sites and localized electronic states within the forbidden band. Furthermore, the high polarizability of Bi^{3+} and La^{3+} ions enhance electronic disorder near the band edges, which facilitates the reduction in both direct and indirect band gaps. These results demonstrate that the optical properties of LB glasses can be effectively tuned through compositional modification, making them suitable for potential optical and photonic applications [26].

Figure 7. shows the photoluminescence (PL) emission spectra of LB glass samples. All samples exhibit broad and intense emission bands, confirming the luminescent nature of the LB glass system. The broadness of the emission bands is characteristic arises from strong electron-phonon coupling and structural disorder within the glass network. A strong and broad emission band is observed in the near-ultraviolet to blue region, extending approximately from 330 to 480 nm, with maximum intensity around 375-425 nm. This emission is attributed to host-related luminescence originating from charge transfer transitions associated with borate structural units and oxygen related defect centers. Similar near UV and blue emissions reported in lanthanum doped borate glasses are commonly associated with the recombination of self trapped excitons, oxygen vacancy centers, and NBO sites formed due to network modification. The increasing lanthanum content

from 0 mol% to 2.0 mol%, noticeable variations are observed in emission intensity. The addition of La^{3+} ions alter the local glass structure by increasing the non-bridging oxygen concentration and defect-related luminescent centers, thereby influencing the emission intensity. Dominant ultra violet-blue emission (330-480 nm), a weaker green emission band (553 nm) were observed, which is attributed to defect-related localized electronic states introduced within the band gap due to structural disorder and the presence of heavy metal ions. A low-intensity red emission (650 nm) is attributed to oxygen vacancy related recombination, while a very weak near-infrared band (825 nm) arises from deep trap levels. The photoluminescence results demonstrate that compositional modification in LB glasses effectively tunes defect-related luminescence without altering the fundamental emission mechanism, highlighting their potential for ultra violet-blue photonic applications such as optical coatings, scintillators, and solid-state lighting hosts [27-29].

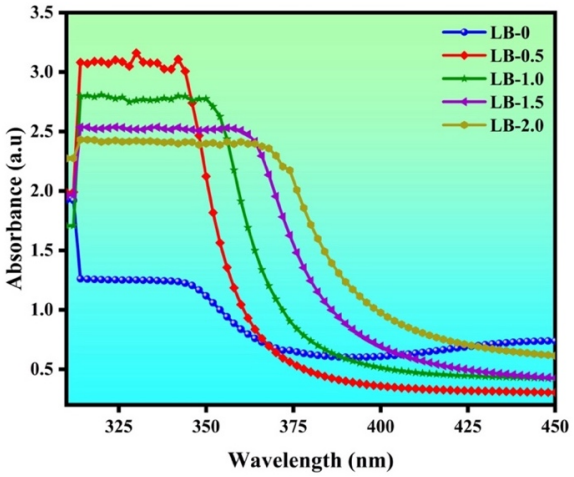

Figure 6. *Optical absorption spectra of LB glass samples*

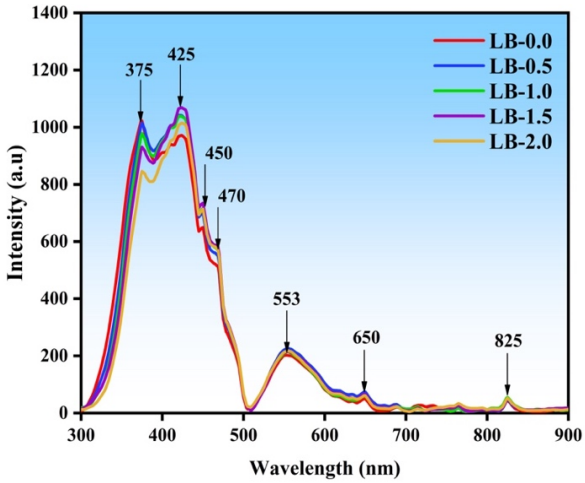

Figure 7. *Emission spectra of LB glass samples*

4. Conclusion

Rare earth infused borobismuth glasses were successfully synthesized by the melt-quenching experimental method, and their structural, physical, optical, and photoluminescence properties were systematically investigated. Amorphous nature of the glasses was confirmed by the X-ray diffraction and raman spectra revealed the presence of BO_3 and BO_4 structural units and the formation of non-bridging oxygen sites due to Bi_2O_3 and La_2O_3 incorporation. Physical and optical properties such as density, refractive index, electronic polarizability, optical basicity, and dielectric constant showed a systematic improvement with increasing dopant concentration, while transmission, metallization, optical electronegativity, and optical band gap decreased because of structural disorder and the creation of localized electronic states. Photoluminescence studies exhibited broad ultraviolet blue emission band, originating mainly from host-related defect centers and NBO sites. The emission intensity was enhanced at lower lanthanum concentrations due to improved local structural asymmetry and polarization effects, whereas concentration quenching occurred at higher levels because of increased non-radiative energy transfer. These findings show a clear correlation between composition, structure, and luminescence behavior, highlighting the

potential of rare earth infused borobismuth glasses for UV blue photonic devices, solid-state lighting, and advanced optical applications**.**

Acknowledgement:
The authors gratefully acknowledge the financial support provided by the Vision Group on Science and Technology (VGST), Government of Karnataka, under the KSTEPS/VGST/ECRA/GRD scheme (Grant No. 1251/2023–24).

References:

1. P. Yasaka, N. Pattanaboonmee, H. J. Kim, P. Limkitjaroenporn, J. Kaewkhao, Gamma radiation shielding and optical properties measurements of zinc bismuth borate glasses. Annals of Nuclear Energy. **68**, 4–9 (2014). https://doi.org/10.1016/j.anucene.2013.12.015
2. I. Boukhris, I. Kebaili, M. S. Al-Buriahi, B. Tonguc, M. M. AlShammari, M. I. Sayyed, Effect of bismuth oxide on the optical features and gamma shielding efficiency of lithium zinc borate glasses. Ceramics International. **46**(14), 22883–22888 (2020). https://doi.org/10.1016/j.ceramint.2020.06.061
3. A. K. Varshneya, Fundamentals of Inorganic Glasses. Elsevier, Amsterdam (2013)
4. M. B. Volf, Chemical approach to glass. Glass Science and Technology. **7**, 465–469 (1984).
5. V. Dimitrov, T. Komatsu, Electronic polarizability, optical basicity and non-linear optical properties of oxide glasses. Journal of Non-Crystalline Solids. **249**(2–3), 160–179 (1999). https://doi.org/10.1016/S0022-3093(99)00317-8
6. X. Zhao, X. Wang, H. Lin, Z. Wang, Correlation among electronic polarizability, optical basicity and interaction parameter of Bi_2O_3–B_2O_3 glasses. Physica B: Condensed Matter. **390,** (1–2), 293–300 (2007). https://doi.org/10.1016/j.physb.2006.08.047
7. S. P. Singh, R. P. S. Chakradhar, J. L. Rao, B. Karmakar, EPR, FTIR, optical absorption and photoluminescence studies of Fe_2O_3 and CeO_2 doped ZnO–Bi_2O_3–B_2O_3 glasses. Journal of Alloys and Compounds. **493**(1–2), 256–262 (2010).
8. K. El-Egili, Infrared studies of Na_2O–B_2O_3–SiO_2 and Al_2O_3–Na_2O–B_2O_3–SiO_2 glasses. Physica B: Condensed Matter. **325**, 340–348 (2003).
9. T. Inoue, T. Honma, V. Dimitrov, T. Komatsu, Approach to thermal properties and electronic polarizability from average single bond strength in ZnO–Bi_2O_3–B_2O_3 glasses. Journal of Solid State Chemistry. **183**(12), 3078–3085 (2010). https://doi.org/10.1016/j.jssc.2010.10.027
10. J. Ahlawat, S. Pawaria, M. Bala, S. Dahiya, A. Ohlan, R. Punia, A. S. Maan, Study of thermal and physical properties of sodium modified zinc borate glasses. Materials Today: Proceedings. **79**, 118–121 (2023). https://doi.org/10.1016/j.matpr.2022.09.523
11. G. A. Alharshan, M. I. Elamy, S. A. Said, A. M. A. Mahmoud, R. A. Elsad, I. M. Nabil, N. M. Ebrahem, Effect of lanthanum oxide on the radiation-shielding, dielectric, and physical

properties of lithium zinc phosphate glasses. Radiation Physics and Chemistry. **224**, 112053 (2024). https://doi.org/10.1016/j.radphyschem.2024.112053

12. M. F. Faznny, M. K. Halimah, M. N. Azlan, Effect of lanthanum oxide on optical properties of zinc borotellurite glass system. Journal of Optoelectronics and Biomedical Materials. **8**(2), 49–59 (2016).
13. A. A. Abul-Magd, A. S. Abu-Khadra, A. M. Taha, A. A. H. Basry, Influence of La^{3+} ions on the structural, optical and dielectric properties and ligand field parameters of Fe^{3+} hybrid borate glasses. Journal of Non-Crystalline Solids. **599**, 121981 (2023). https://doi.org/10.1016/j.jnoncrysol.2022.121981
14. M. Bala, S. Agrohiya, S. Dahiya, A. Ohlan, R. Punia, A. S. Maan, Effect of replacement of Bi_2O_3 by Li_2O on structural, thermal, optical and other physical properties of zinc borate glasses. Journal of Molecular Structure. **1219**, 128589 (2020). https://doi.org/10.1016/j.molstruc.2020.128589
15. A. D. Sontakke, K. Biswas, A. Tarafder, R. Sen, K. Annapurna, Broadband Er^{3+} emission in highly nonlinear bismuth modified zinc-borate glasses. Optical Materials Express. **1,** (3), 344–356 (2011). https://doi.org/10.1364/OME.1.000344
16. Sayyed, M. I., Alshamari, A., & Mhareb, M. H. A. (2025). Roles of ZnO and La2O3 in enhancing the mechanical, optical, and radiation shielding properties of B2O3-Bi2O3-Na2O transparent glasses. *Journal of Radiation Research and Applied Sciences*, *18*(4), 101859. https://doi.org/10.1016/j.jrras.2025.101859
17. Zakaly, H. M., Abouhaswa, A. S., Issa, S. A., Mostafa, M. Y., Pyshkina, M., & El-Mallawany, R. (2020). Optical and nuclear radiation shielding properties of zinc borate glasses doped with lanthanum oxide. *Journal of Non-Crystalline Solids*, *543*, 120151. https://doi.org/10.1016/j.jnoncrysol.2020.120151
18. Hassaan, M. Y., Saudi, H. A., Gomaa, H. M., & Morsy, A. S. (2020). Optical properties of bismuth borate glasses doped with zinc and calcium oxides. *Journal of Materials and Applications*, *9*(1), 46-54. https://doi.org/10.32732/jma.2020.9.1.46
19. Terashima, K., Tamura, S., Kim, S. H., & Yoko, T. (1997). Structure and nonlinear optical properties of lanthanide borate glasses. *Journal of the American Ceramic Society*, *80*(11), 2903-2909.
20. Padmaja, G., & Kistaiah, P. (2009). Infrared and Raman spectroscopic studies on alkali borate glasses: evidence of mixed alkali effect. *The Journal of Physical Chemistry A*, *113*(11), 2397-2404.
21. Abouhaswa, A. S., & Kavaz, E. (2020). Bi2O3 effect on physical, optical, structural and radiation safety characteristics of B2O3Na2O-ZnOCaO glass system. *Journal of Non-Crystalline Solids*, *535*, 119993.
22. Bhatia, B., Meena, S. L., Parihar, V., & Poonia, M. (2015). Optical basicity and polarizability of Nd3+-doped bismuth borate glasses. *New Journal of Glass and Ceramics*, *5*(3), 44-52. http://dx.doi.org/10.4236/njgc.2015.53006

23. Alotaibi, B. M., Alhuzaymi, T. M., Alotiby, M., Makhlouf, S., Shaaban, K. S., & Abdel Wahab, E. A. (2024). Electronegativity, susceptibility, and radiation shielding features of thulium reinforced barium-cadmium-lithium-borate glasses. *Chalcogenide Letters*, *21*(8).
24. Chethan, M., Reddy, M. S., Abhiram, J., & Rajiv, A. (2020, March). Optical properties of calcium sodium phosphate glasses doped with strontium. In *Journal of Physics: Conference Series* (Vol. 1495, No. 1, p. 012030). IOP Publishing. doi:10.1088/1742-6596/1495/1/012030
25. Hamad, M. K., Sayyed, M. I., Mhareb, M. H. A., Sadeq, M. S., Dwaikat, N., Almessiere, M. A., & Ziq, K. A. (2022). Effects of TiO2, V2O5, MnO2 and Tl2O3 on structural, physical, optical and ionizing radiation shielding properties of strontium boro-tellurite glass: an experimental study. *Optical Materials*, *127*, 112350. https://doi.org/10.1016/j.optmat.2022.112350
26. Alharshan, G. A., Elamy, M. I., Ebrahem, N. M., Mahmoud, A. M. A., Rammah, Y. S., Rammah, R. A., Elsad, M., Hamed Misbah, and Shimaa Ali Said. (2024). Physical, structural, and optical characteristics of the glasses system based on lanthanum-doped phosphate. *Optical and Quantum Electronics*, *56*(7), 1179. https://doi.org/10.1007/s11082-024-07160-6
27. Erol, E., Vahedigharehchopogh, N., Kıbrıslı, O., Ersundu, M. Ç., & Ersundu, A. E. (2021). Recent progress in lanthanide-doped luminescent glasses for solid-state lighting applications-A review. *Journal of Physics: Condensed Matter*, *33*(48), 483001. https://doi.org/10.1088/1361-648X/ac22d9
28. Yasaka, P., & Kaewkhao, J. (2015, November). Luminescence from lanthanides-doped glasses and applications: A review. In *2015 4th International Conference on Instrumentation, Communications, Information Technology, and Biomedical Engineering (ICICI-BME)* (pp. 4-15). IEEE.
29. Jarucha, N., Wantana, N., Kim, H. J., Wongdamnern, N., Sareein, T., & Kaewkhao, J. (2022). Physical, optical and luminescence properties of Pr3+ doped in lanthanum borate glasses. *Integrated Ferroelectrics*, *222*(1), 253-261. https://doi.org/10.1080/10584587.2021.1961537